Received: 29 January 2025 | Accepted: 10 July 2025

DOI: 10.1111/1365-2435.70148

Functional Ecology

RESEARCH ARTICLE

Imposing primary colonisation success of wood-decomposing fungi in birch wood alters microbiome composition and carbon release rates

Aiym Bakytbaikyzy | Yanmei Zhang | Collin Adams | Jonathan S. Schilling

Department of Plant and Microbial Biology, University of Minnesota, Saint Paul, Minnesota, USA

Correspondence
Jonathan S. Schilling
Email: schillin@umn.edu

Funding information
Minnesota's Discovery, Research, and InnoVation Economy (MnDRIVE) Environment Graduate Scholar Seed Grant Award; John Tester Itasca Research Fellowship

Handling Editor: Anita Risch

Abstract

1. Fungi dominate the decomposition of deadwood, with white rot-type species removing more lignin than brown rot-type species to gain access to wood carbohydrates. These fungi often compete to colonise the same tree species, and globally, a small shift in the success of either rot type could have massive greenhouse gas implications.
2. For this reason, we need to know what controls white vs. brown rot outcomes, starting with field studies that track fungi and the fate of wood lignin under real-world conditions. Such experiments, however, have had skewed, white-rot-only outcomes and have lacked representation of bacteria that compete for wood sugars.
3. To address this, we pre-inoculated small-diameter birch *Betula papyrifera* stem sections with a brown rot fungus *Fomitopsis betulina* and compared these to non-inoculated birch in a treatment design that had been dominated by white rot fungi in past field studies.
4. This approach encouraged more brown rot, widening the range of wood physico-chemical outcomes (density, pH, lignin and carbohydrate profiles).
5. Achieving the brown rot outcome allowed us to better connect the fungal rot type as a trait to its functional outcomes. Specifically, it enabled us to test for definitive links between dominant fungi (identified via ITS2 amplicon sequencing), their C release patterns, and their bacterial associates (identified via 16S rRNAV4 amplicon sequencing). We observed a clear link between rot type and fungal dominance but did not find parallel bacterial codominance. While the Shannon index for fungi was lower in brown-rotted wood than in white-rotted wood, the pattern was reversed for bacteria. Bacterial beta diversity, too, was different between brown- and white-rotted wood. This fungal influence on bacterial diversity may be due to increased niche space (i.e., higher availability of soluble sugars) for bacteria when brown rot fungi dominate.

This is an open access article under the terms of the Creative Commons Attribution License, which permits use, distribution and reproduction in any medium, provided the original work is properly cited.
© 2025 The Author(s). *Functional Ecology* published by John Wiley & Sons Ltd on behalf of British Ecological Society.

6. Collectively, achieving these more directed wood rot-type outcomes enabled us to clearly link fungal dominance to wood physicochemical changes, including C release, while also revealing a lack of relationship between dominant fungi and the success of associated bacteria.

KEYWORDS
brown rot, endophyte, fungi, lignocellulose, microbial community, priority effects, white rot, wood decomposition

1 | INTRODUCTION

Accurate prediction of carbon (C) fluxes from wood decomposition is a critical gap in modelling greenhouse gas emissions (Keenan et al., 2013). Trees sequester 80% of Earth's aboveground C in their secondary xylem (i.e., wood) (Houghton et al., 2009), which contains lignin, cellulose and hemicellulose (Chen, 2014). Classic plant trait predictors of decomposition (e.g., C:N; lignin content) fail to explain much of the variability in wood decay at local scales (Van Der Wal et al., 2015). Instead, microbial community assembly can 'steer' a single tree species under similar environmental conditions towards very different outcomes (Cline et al., 2018; Fukami et al., 2010; Song et al., 2017). These alternate pathway options are due to fungi that dominate the biological decomposition of wood and govern C desequestration, either reallocating C to the soil or releasing it to the atmosphere (Floudas et al., 2012; Rayner & Boddy, 1988). Wood-decomposing fungi are not functionally redundant: they have a spectrum of traits that vary C release and can frustrate trait–function correlations (Dickie et al., 2012; Lodge, 1997).

Some of these fungal traits explain variability in the *rates* of C released during wood decomposition, including host-specificity, metabolic rates and life-history strategies. The fungi that variably dominate wood decomposition are, on average, less host-specific than other fungal litter decomposers (Lodge, 1997). Although there are examples of host-specificity (e.g., *Fomitopsis betulina* on birch), community assembly in a given deadwood log is generally more flexible—colonisation timing (Dickie et al., 2012; Fukami et al., 2010) and inoculum potential (Song et al., 2015) both matter. The fungi that rise to dominance also have variable growth habits and combative capacities that can hasten or stall decay. For example, 27% of the variability in fungal wood decay, measured as wood mass loss, was found to be positively correlated with one trait—hyphal extension rate (Lustenhouwer et al., 2020). Conversely, fast-growing but non-lignolytic *Trichoderma* spp. are combative enough to stall decay for long periods of time if arriving as early colonisers (Schubert et al., 2008) or as mycoparasites of other early-colonising fungi (Kubicek et al., 2011).

Variability in the *fates* of wood C, however, can be explained by a different trait—fungal rot type (i.e., 'nutritional mode'). Fungi have different strategies for deconstructing lignocellulose, and these vary CO_2 release. White rot fungi access cellulose and hemicellulose by attacking the lignin barrier using Class II peroxidases (Floudas et al., 2012) and depolymerising or decoupling phenylpropane units (Blanchette, 2003). White rot fungi dominate wood decomposition in temperate, higher latitude forests (>80% taxonomically (Gilbertson, 1980) and in collections (Simpson et al., 2024)), and their lignin selectivity and thus C release vary among species (Stokland & Alfredsen, 2024; Worrall et al., 1997). In contrast, brown rot fungi, which are most commonly found in high-latitude and high-altitude conifer forests (Simpson et al., 2024), circumvent lignin. Brown rot fungi use reactive oxygen species (ROS) to selectively extract sugars from cellulose and hemicellulose (Arantes & Goodell, 2014; Floudas et al., 2012). Brown rot fungi leave more lignin behind in woody residues than white rot fungi and likely sequester more C into the soil (Stokland & Alfredsen, 2024). However, similarly to white rot fungi, brown rot fungi vary in how much lignin they remove (Schilling et al., 2020; Stokland & Alfredsen, 2024; Stutz et al., 2017, 2019) or modify (Yelle et al., 2008).

This spectrum of fungal-derived fates for lignin-bound C (40% of wood C) creates, we assume, a spectrum of C emissions (Martin et al., 2021). Shifts of average C emission along this spectrum could have major global consequences. In a warming world, the higher-latitude and higher-altitude distributions of brown rot fungi seem likely to contract, releasing more C from lignin as both white rot fungi and white-rot-associated microbes that release C from lignin expand. This could create positive feedback between CO_2 emissions and warming, and with 146 Gt of global C in lignin (Friedlingstein et al., 2022; Houghton et al., 2009), a small contraction in brown rot could release an immense amount of CO_2 equivalents from lignin.

We need to know what controls these white vs. brown rot outcomes to be able to predict future wood C fates. A specific need is field studies that track fungi and the fate of wood lignin under real-world conditions, but these have had only white rot as an outcome (e.g., Cline et al., 2018) and have lacked representation of bacteria that compete with fungi for wood carbohydrates. Bacteria have a low capacity to decay sound wood (de Boer et al., 2005; Johnston et al., 2016), but many have the basic capacity to metabolise lignocellulosic oligomers (López-Mondéjar et al., 2016; Salvachúa et al., 2015), and their co-colonisation of wood could shape niche spaces for wood-colonising fungi, and vice versa (Christofides et al., 2019; Folman et al., 2008; Murray & Woodward, 2003; Tláskal et al., 2021). As a case in point, during brown rot, concentrations of soluble sugars are higher than in white-rotted wood (Cowling, 1961;

Schilling et al., 2020), likely as a consequence of non-targeted carbohydrate depolymerisation via ROS. We assume more C is sequestered into the soil during brown rot, but evidence is indirect (Stokland & Alfredsen, 2024), and bacteria may metabolise some/all of these sugars. Wood-decaying fungi may further shape niche spaces for bacteria by altering pH (Jurgensen et al., 1989; Song et al., 2017), secreting consumable by-products (Stopnisek et al., 2016), and/or directly antagonising or facilitating bacteria (Janeš et al., 2006; Pierce et al., 2021; Rousk et al., 2008; Stopnisek et al., 2016). Conversely, bacteria could shape the niche spaces for coloniser fungi (Jurgensen et al., 1989; Murray & Woodward, 2003), including 'cheaters' (Allison, 2005), who may decrease the metabolic payoff from fungal-secreted enzymes or reduce the benefits of an ROS mechanism that is too productive in releasing soluble sugars.

To establish the link between fungal decomposition traits and their functional consequences in a field wood-decay study, we attempted to broaden the range of outcomes to include brown rot in a study system that we knew was biased for white rot (Cline et al., 2018; Maillard et al., 2022). Specifically, we inoculated small-diameter birch *Betula papyrifera* stem sections with a birch-specific brown rot fungus *Fomitopsis betulina* (Pleszczyńska et al., 2017), and compared these with non-inoculated sections placed in ground contact for 14 months. Given the wide boreal distribution of *B. papyrifera* (Apps et al., 1993; Kneeshaw & Gauthier, 2003), and the host-specificity of *F. betulina* (Henningsson, 1965) among many potential white rot fungal colonisers of birch (Gilbertson, 1980), we hypothesised that we could constrain decay stage and force a broader range across brown vs, white rot outcomes. We also hypothesised that this could establish clearer links between dominant fungi, their C release patterns, and the possible codominance of bacteria shaped by (or shaping) fungal success.

2 | MATERIALS AND METHODS

2.1 | *Fomitopsis betulina* solid-state inoculum preparation

We adapted techniques used for inoculating logs for edible mushroom cultivation to control the inoculum potential of *Fomitopsis betulina* (formerly *Piptoporus betulinus*), a non-edible fungus. The *F. betulina* strain was isolated from the University of Minnesota Cloquet Experimental Forest; it was verified by ITS2 sequencing and is publicly available in the University of Minnesota Forest Pathology culture collection.

To create inoculum 'spawn', five canning jars were filled two-thirds with whole oats and submerged in distilled water overnight. After soaking, excess water was strained and oats were air-dried for 3 h. Oats were autoclaved for 1 h (121°C; 16 psi), rested for 48 h and autoclaved again for 1 h. Cooled jars of oats were each inoculated with 4 agar plugs (0.7 cm diameter) from the edge of *F. betulina* mycelium (grown on potato dextrose agar) and incubated (26°C; 70% relative humidity) for 3 weeks until thoroughly colonised.

Twelve *B. papyrifera* trees, each over 10 years old and with a base diameter >4 cm (exceeding the 'coarse woody debris' threshold (Harmon et al., 2004)), were cut from our study site north of Itasca Biological Station and Laboratories (IBSL) (47.250471 N; 95.228816 W). We did not need permission for this fieldwork. Bark-free sawdust (Wiley-milled to 20-mesh) was acquired from stem sections >3 cm in diameter from two of the 12 trees. Five canning jars with 375 g of pre-soaked sawdust were autoclaved twice for 1 h with a 48-h resting period, as above for oats. A 2-cm top layer of colonised oats was added to each jar of sawdust and gently mixed. Jars were incubated for 3 weeks, as above for oats.

2.2 | Field experiment

Eight replicate birch stem sections (12 cm length; 3–4 cm diameter, knot-free) for eight treatments, plus a non-decayed control (4 cm length) cut from each tree yielded 72 birch stem sections in total from eight out of ten trees not used for sawdust (Figure S1). Eight sections were cut and assigned to treatments (Table S1) so that each tree had one of each treatment, and each treatment had one of each stem position (base section, second from base, and so forth). Non-decayed control sections were located in the middle (fifth from base). Holes at both ends of all stem sections, except controls, were drilled to a 12.5 mm depth, using an angle grinder at RPM >2400 and a soft-steel, screw-tip bit with a stop-collar (Figure S1). Excepting controls, every other section per tree was then autoclaved for 1 h to sterilise half of the treatment sections (Figure S1). In parallel, soil collected from the upper 10 cm adjacent to cut trees was homogenised and divided, with one of the two bags autoclaved for 1 h, as above. Stem holes were inoculated using a traditional inoculation tool jabbed once into either sawdust colonised by *F. betulina* or sterile birch sawdust (Figure S1). Melted paraffin wax was used to seal each hole. The last two birch trees were cut into eight stem sections each, and these 16 sections were used as sacrificial samples to time the final sampling. Sacrificial samples were placed only on non-sterilised soil, so represented a subset of the fully factorial design (i.e., included four of the eight possible treatments, in which only wood sterility and inoculum presence were varied).

In August 2021, an 8×10 grid was created at the study site, an early-successional forest of birch *Betula papyrifera*, balsam fir *Abies balsamea* and aspen *Populus tremuloides*. Grid spacing was 30 cm between rows and columns. At each grid point, 500 mL of sterilised or non-sterilised soil was added and tamped to create a circular pad, alternating in a checkerboard pattern to ensure no same-treatment soil was adjacent in rows or columns. Wood treatments (sterilised vs. non-sterilised; inoculated vs. non-inoculated) were placed in ground contact across this grid on top of the soil (sterilised vs. non-sterilised) pads, with cut ends facing East–West. Small U-shaped galvanised stakes secured them in ground contact, free of fallen leaves. Treatments were spaced to avoid adjacency of the same type. Two extra columns contained the 16 sacrificial stem sections that were destructively harvested to track decay progress and to time final

sampling. The study site was enclosed using waist-height, galvanised hexagonal fencing to minimise disturbance by animals.

2.3 | Harvesting decayed samples

When density loss in sacrificial samples reached decay classes II–III (Harmon et al., 2008) in 14 months, all stems were harvested. Inoculation holes containing the 12.5 mm inoculation spawn were removed using a band saw sprayed with 70% ethanol between cuts. Bark was removed from the remaining centre sections, and each was cut longitudinally, parallel to the grain and in a manner that ensured both halves contained the part of the wood that had been in contact with soil (Figure S1). One half-cylinder was used for DNA analyses, and the other half-cylinder was used for wood physicochemical characterisation.

2.4 | Wood physicochemical characterisation

To measure wood density, fresh wood volume was measured via water displacement, and dry wood mass was measured after drying at 100°C for 48 h. Density loss was calculated relative to non-decayed controls. Samples were then Wiley-milled to 20 mesh. Acid-insoluble components of the resulting wood sawdust were measured gravimetrically as Klason lignin, using 72% sulphuric acid as a solvent and without subtracting ash contents that are minuscule in birch (Pettersen, 1984; Schilling et al., 2020). Lignin concentrations were adjusted to compensate for the illusion of gain—caused by the loss of other components—by multiplying each value by the fraction of the density remaining (decayed wood density vs. sound/non-decayed wood density) (Anderson et al., 2023), and lignin loss was calculated as a percentage. Lignin loss was paired with density loss as a ratio (L:D) and used as a rot-type indicator (<0.8 for brown rot; >0.8 for white rot) (Worrall et al., 1997), which has been confirmed among 79 species (Schilling et al., 2020). Acid-soluble sugars (glucose, xylose, galactose, arabinose and mannose) were quantified via high-performance liquid chromatography (HPLC) using an Aminex HPX-87P Carbohydrate Analysis Column and Biorad De-Ashing Micro-Guard Cartridges. Mobile phase was HPLC-grade water at an operating flow rate of 0.6 mL min^{-1}. The column thermostat was set to 85°C and refractive index (at 35°C) was used for detection. Standard curves were acquired using reagent-grade glucose, xylose, galactose, arabinose and mannose. For each sample, the concentrations of glucose, xylose, galactose, mannose and arabinose monosaccharides were derived from the area under each sugar's peak. Monosaccharide amounts were calculated by multiplying monosaccharide concentrations by the total reaction volume. Then, monosaccharide amounts were multiplied by each sugar's hydration factor to get the amounts of structural carbohydrates. Then, the percent of structural carbohydrates was calculated as a fraction of the total mass of the starting sample material. Finally, the percentage of structural carbohydrates was adjusted for density loss by multiplying the percentage of structural carbohydrates by the fraction of the density remaining in each sample (decayed wood density vs. non-decayed wood density) (Anderson et al., 2023; Schilling et al., 2020).

2.5 | DNA extraction and sequencing

Half-cylinder stem sections reserved for DNA analyses were stored at −80°C until processing. Drill bits (0.635 cm in diameter) and metal spatulas were sterilised at 180°C for 3 h. Samples were drilled, while frozen, using established spacing and sterile techniques (Zhang et al., 2024). Qiagen (Hilden, Germany) DNeasy PowerLyzer PowerSoil Kit was used for extracting DNA from 200 to 400 mg of sawdust using the modified protocol (Zhang et al., 2024). The extracted DNA's concentrations and purity were checked using the Qubit fluorometer and gel electrophoresis. Extracted DNA was analysed by the University of Minnesota Genomics Center using MiSeq 2×300 (Illumina, San Diego, CA, USA) amplicon sequencing, targeting ITS2 and 16S rRNA V4 genes (Table S2) (Gohl et al., 2016; Zhang et al., 2024).

2.6 | Replication statement

Scale of inference	Scale at which the factor of interest is applied	Number of replicates at the appropriate scale
Tree	Tree	8
Individual stem section	Individual stem section	8 of each combination; 64 total decayed
Individual stem section	Individual stem section	8 non-decayed

2.7 | Data processing and statistical analyses

Statistical analyses and data visualisation were performed on R and considered significant at $p \leq 0.05$. Differences in (1) surface-area-to-volume ratio of wood samples post-decay (Figure S2), (2) wood density loss and (3) L:D of samples by wood treatment (sterilised vs. non-sterilised), soil treatment (sterilised vs. non-sterilised) and inoculum treatment (inoculated vs. non-inoculated) were assessed using three-way factorial analysis of variance (ANOVA). Prior to running ANOVA, variance homoscedasticity and normality of residuals were confirmed using Levene's and Shapiro–Wilk's tests. Differences in pH, structural carbohydrates and Klason lignin concentrations across treatment groups were assessed using the Wilcoxon non-parametric test.

Amplicon sequences received as raw demultiplexed .fastq files were processed using the DADA2 pipeline (Callahan et al., 2016). Fungal and bacterial amplicon sequence variants (ASVs) were

assigned using the UNITE general FASTA release for eukaryotes Version 18.07.2023 (Abarenkov et al., 2024) and Silva 138 SSU Ref NR 99 (Quast et al., 2013), respectively. The ASVs assigned to the *Fomitopsis* genus with a species assignment 'NA' were examined via BLAST (Altschul et al., 1990) and verified to be *Fomitopsis betulina* (97.41%–99.74% identity; E-values ranging $0–5\times10^{-165}$). Based on assigned taxonomy, fungal ASVs were classified into ecological groups using the FungalTraits database (Põlme et al., 2020). Non-fungal and non-bacterial taxa, as well as taxa labelled as 'NA' at the kingdom level, were removed. ASVs with <10 reads in a given sample, and samples with <100 fungal/bacterial reads were also removed (=2 fungal samples; =6 bacterial samples). For non-decayed samples, 94% of reads were removed as non-fungal ASVs, with 92% belonging to the tree host. Similarly, 99.8% of reads from the non-decayed samples were removed as non-bacterial. Given differences in read depth, rarefications of fungal and bacterial alpha diversities were performed separately for non-decayed and decayed samples. The rarefaction depth for fungi in decayed samples was set to 10,000 and to 100 in non-decayed samples. For bacteria, the rarefaction depth was set to 14,000 and 608 in decayed and non-decayed samples, respectively.

ASV richness, as well as Shannon and Pielou evenness indices were calculated using the 'microbiome' package (Lahti & Shetty, 2017). Faith phylogenetic diversity (PD) index was calculated using the 'picante' package (Kembel et al., 2010). Effects of soil sterilisation, wood sterilisation, and pre-inoculation with *F. betulina* on each of the four alpha diversity metrics were tested using the Wilcoxon non-parametric test. To visualise treatment effects on community composition, we generated non-metric multidimensional scaling plots, after calculating Bray–Curtis distances using the 'vegan' package (Oksanen et al., 2017). To examine effects (with interactions) of soil sterilisation, wood sterilisation and pre-inoculation with *F. betulina* on fungal and bacterial community structures, we performed a permutational multivariate analysis of variance using ADONIS2 in the 'vegan' package (Oksanen et al., 2017).

3 | RESULTS

3.1 | Outcomes of wood decay

Inoculum was the only factor affecting density loss (three-way ANOVA; $F_{1,56}=177.3$, $p<0.001$). Mean density loss for inoculated treatments was 44.7%±10.9%, and mean density loss for non-inoculated treatments was 12.7%±8.0% (Figure 1a). To assign rot-type outcomes, wood decay must be above bole decay class I (no longer 'sound') but below class IV (not becoming soil) (Schilling et al., 2015). For birch, this corresponds to density loss values between 9.2% and 45.6% (Harmon et al., 2008). Of 64 decayed samples in our study, 39 (60.9%) were in decay classes II–III (Harmon et al., 2008). We measured lignin loss and paired it with density loss to generate a ratio (L:D) and use it as a rot-type indicator (<0.8 for brown rot, >0.8 for white rot). Limiting statistical analyses to these 39 birch sections, inoculated samples had lower L:D values (0.24±0.37) than non-inoculated samples (1.73±0.57) (Figure 1b; three-way ANOVA; $F_{1,31}=107.8$, $p<0.001$), and samples placed on sterilised soil had lower L:D values (0.790±0.738) than samples placed on non-sterilised soil (1.38±0.99) (Figure 1b; three-way ANOVA; $F_{1,31}=11.8$, $p<0.01$). Most inoculated sections had a brown rot outcome (L:D<0.8), whereas most non-inoculated sections had a white rot outcome (L:D>0.8).

3.2 | Chemistry of decayed wood

Decayed wood (i.e., stem sections that were placed onto the field site and left to decay for 14 months) had significantly lower pH than non-decayed wood (i.e., sound wood/stem sections that were processed as soon as birch trees were cut) (Wilcoxon test; $n_1=8$, $n_2=64$, statistic=12, $p<0.001$) (Figure 1c). Wood inoculated with brown rot *F. betulina* had lower pH than non-inoculated wood (3.0 and 3.5, respectively), with inoculum being the only significant factor (Wilcoxon test; $n_1=32$, $n_2=32$, statistic=7, $p<0.001$) (Figure 1c). Inoculum was also the sole factor affecting adjusted concentrations of Klason lignin and carbohydrates, with samples inoculated with brown rot *F. betulina* containing more residual Klason lignin ($p<0.001$) than non-inoculated samples (Figure 2; Table S3). Conversely, there was less arabinan ($p<0.05$), galactan ($p=0.001$), glucan ($p<0.001$), mannan ($p<0.001$), and xylan ($p<0.001$) in inoculated samples than in non-inoculated samples (Figure 2; Table S3).

4 | FUNGAL AND BACTERIAL COMMUNITY COMPOSITION

Decayed birch had higher fungal richness ($p<0.001$), higher Faith PD index ($p<0.001$) and lower evenness ($p<0.05$) than non-decayed birch (Figure S3A; Table S4), but this comparison has the caveat of read depths mentioned in Section 2. Fungal beta diversity was also different between decayed and non-decayed birch (Figure S4).

Fomitopsis betulina dominated in inoculated samples, in all but one case (sample E2), producing large sporophores and with a mean relative DNA abundance of 84.7%±21.6% (Figure 3a; Figure S5). Non-decayed birch had a ~50% relative abundance of *F. betulina* (Figure 3a), indicating that it was present as an endophyte but was unable to succeed in ground contact in non-inoculated stem sections. Endophytic *F. betulina* read counts in non-decayed birch were low (mean 118±80), compared to decayed birch inoculated with *F. betulina* (mean 49,380±19,521). In non-inoculated decayed birch, white rot fungi dominated (Figure 3b), but the dominant taxa varied according to treatments. When stem sections were pre-sterilised, *Phanerochaete* (mostly spp. *livescens*) and *Sistotrema* (spp. *brinkmannii*, *porulosum* and *coroniferum*) colonised and dominated (Figure 3a). When stem sections had not been pre-sterilised, *Peniophora* (mostly sp. *cinerea*) and *Trametes* (mostly sp. *pubescens* and some sp. *versicolor*) had high relative abundances (Figure 3a),

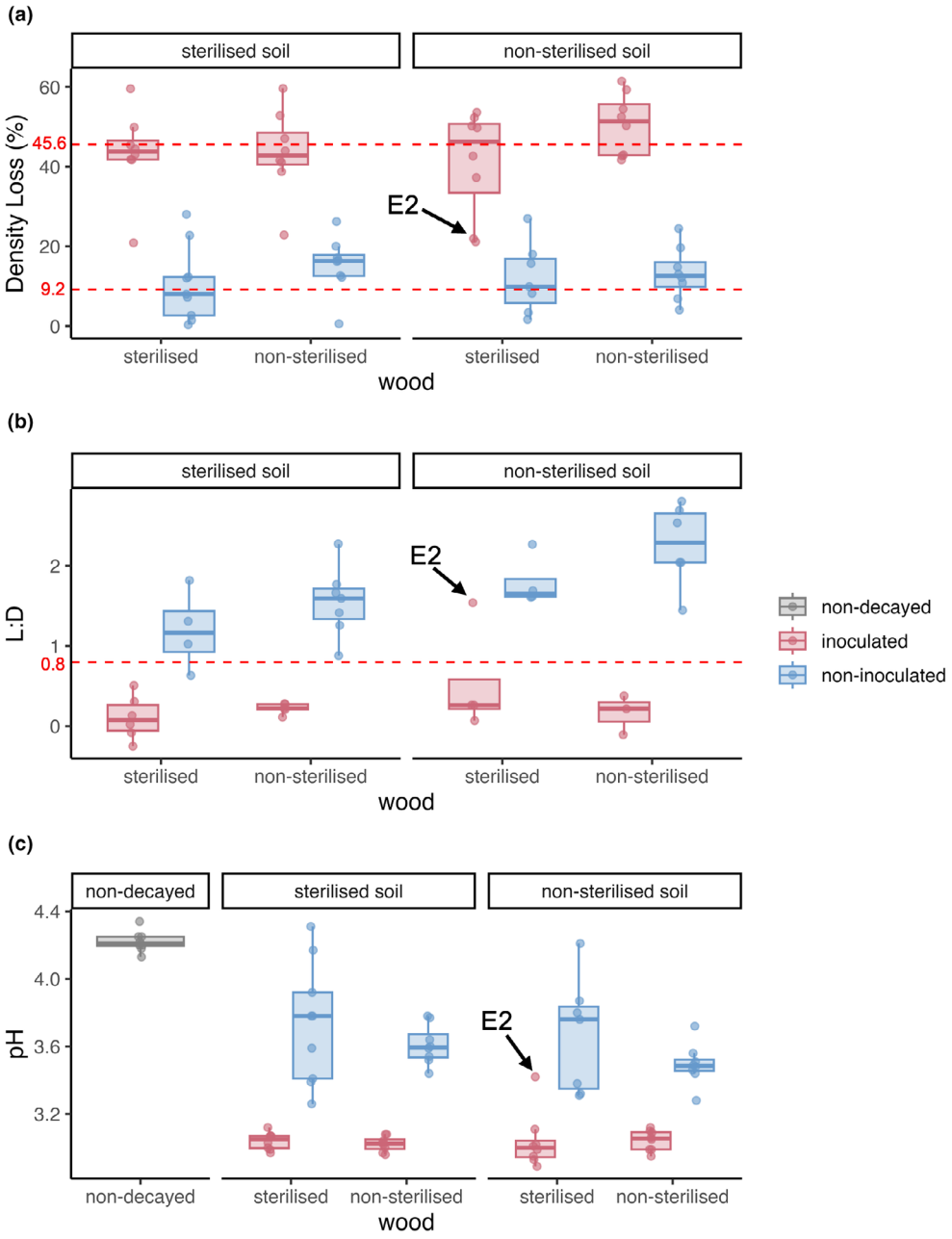


FIGURE 1 Physicochemistry of wood across treatments. (a) Density loss of decayed birch stem sections, relative to non-decayed sections. The red dashed lines indicate the density loss thresholds used to define decay stages II–III (9.2%–45.6%). (b) L:D values of decayed samples in decay stages II–III, showing the 0.8 threshold (red dashed line) for rot type (brown rot L:D < 0.8; white rot L:D > 0.8). (c) Birch wood pH. 'Non-decayed' refers to sound wood. Data for decayed samples are faceted horizontally by the soil variable (sterilised vs. non-sterilised) and coloured by the inoculum variable (inoculated vs. non-inoculated). The wood variable (sterilised vs. non-sterilised) is on the *x*-axes and the density loss, L:D and pH values are on the *y*-axes. The single brown-rot-inoculated sample (E2) that had a white rot fungus rise to dominance is shown, demonstrating the consistency of wood chemistry with fungal dominance.

likely due to their presence and priority as endophytes. In contrast, relative abundances of dominant bacterial species showed no clear taxonomic correlations or differences across treatments (Figure 3c).

Despite differences in fungal community composition between sterilised and non-sterilised wood, inoculation was the only factor significantly affecting fungal alpha diversity. Inoculation did not affect richness, but it lowered Pielou evenness ($p < 0.001$) and Shannon ($p < 0.001$) indices and increased the Faith PD index ($p < 0.001$) (Figure 4a; Table S5). Inoculation was also the only significant variable influencing bacterial alpha diversity. Bacterial richness ($p < 0.005$), Shannon ($p < 0.001$), Pielou evenness ($p < 0.001$) and Faith PD ($p < 0.005$) indices were all higher in brown-rotted than in white-rotted wood ($p < 0.001$) (Figure 4b; Table S5). Inoculation also affected fungal ($R^2 = 0.27$; $Pr(>F) = 0.001$) and bacterial ($R^2 = 0.15$; $Pr(>F) = 0.001$) beta diversities (Figure 5a,b; Table S6). Wood and soil

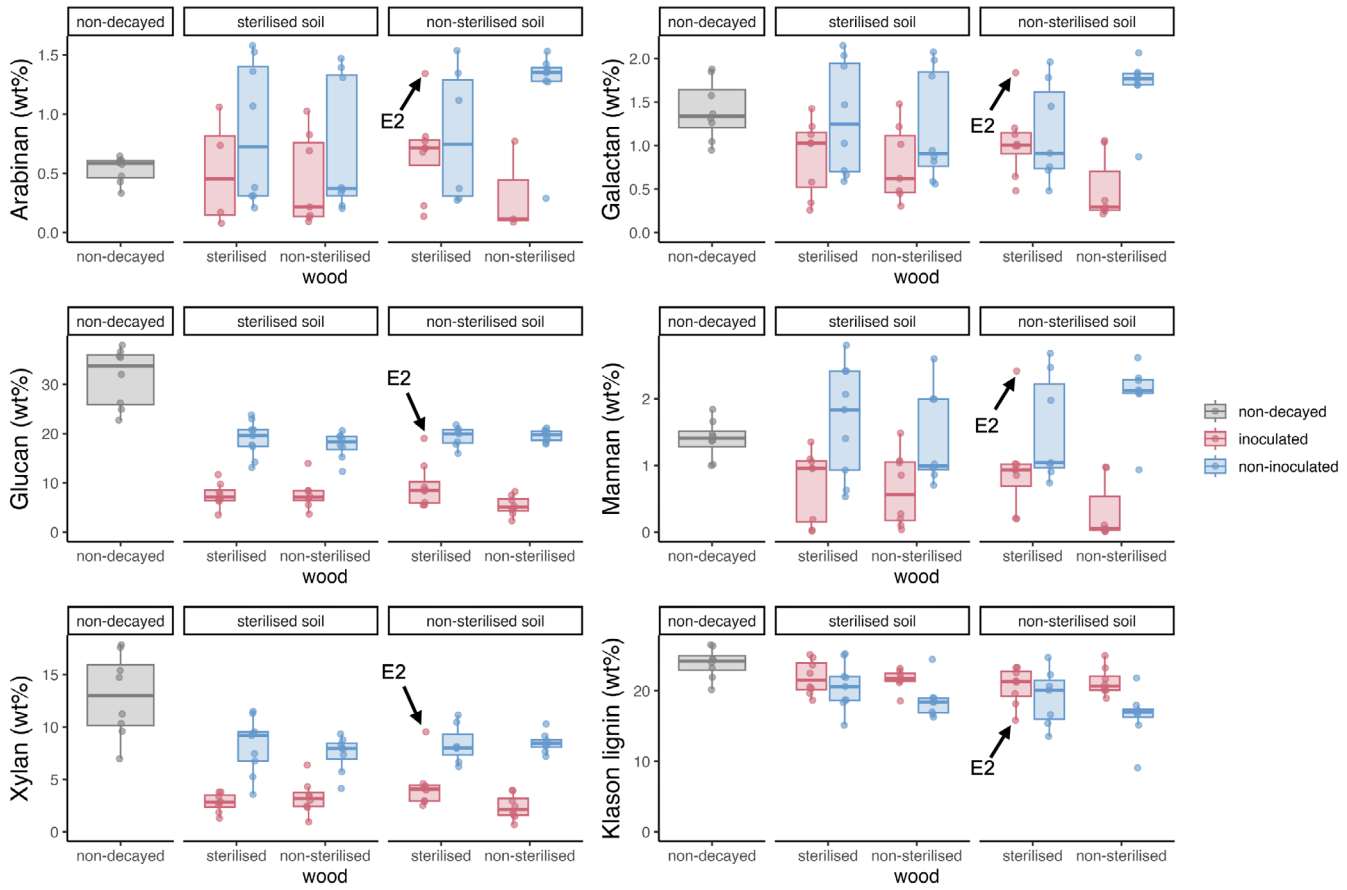


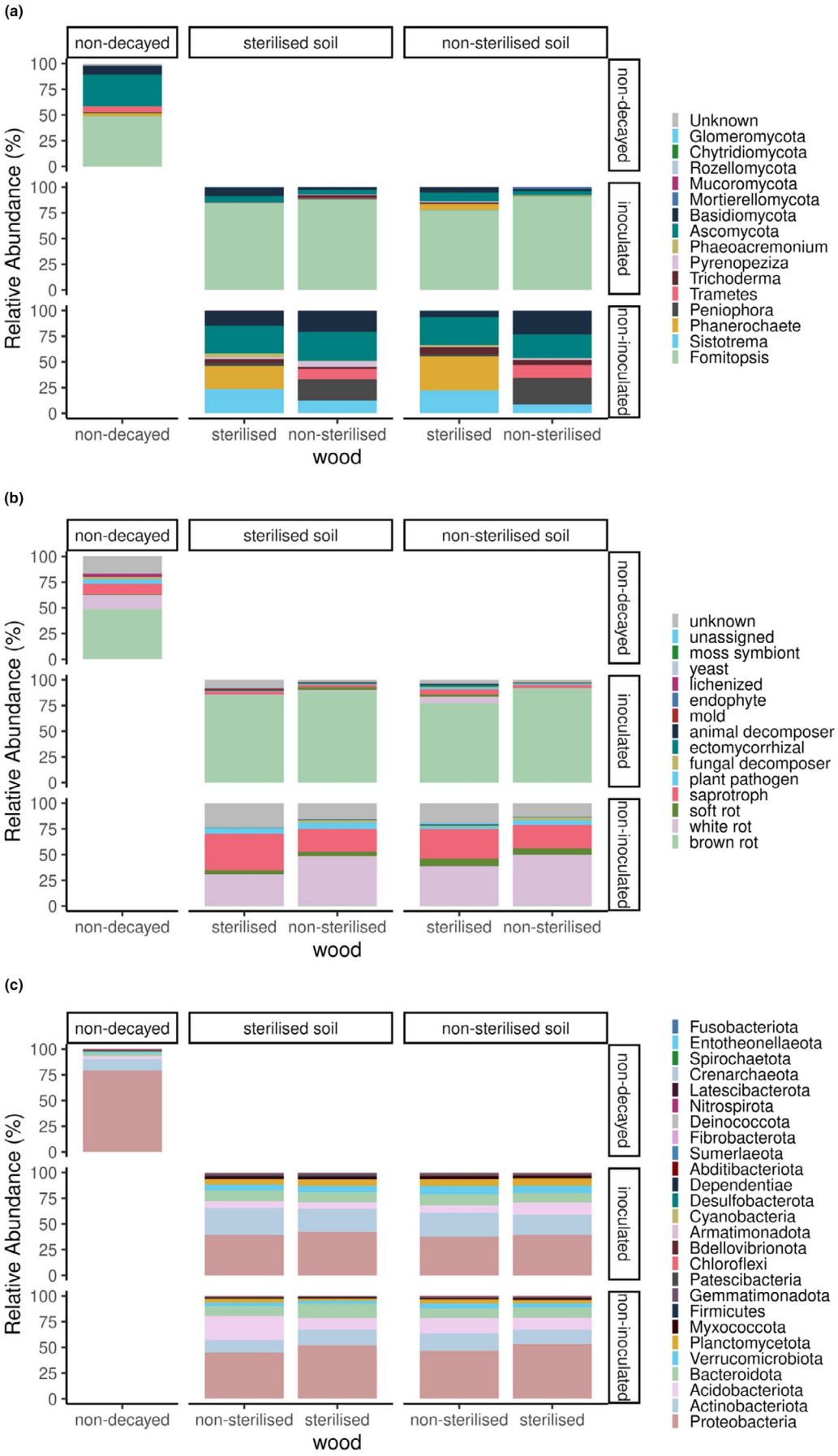
FIGURE 2 Concentrations of structural carbohydrates and Klason lignin in wood, across treatments. 'Non-decayed' refers to sound wood. Data for decayed samples are faceted horizontally by the soil variable (sterilised vs. non-sterilised) and coloured by the inoculum variable (inoculated vs. non-inoculated). The wood variable (sterilised vs. non-sterilised) is on the x-axes and the concentrations (adjusted for density loss) of structural carbohydrates and Klason lignin are on the *y*-axes. The single brown-rot-inoculated sample (E2) that had a white rot fungus rise to dominance is shown, demonstrating the consistency of wood chemistry with fungal dominance.

sterilisation did not affect bacterial beta diversity, but wood sterilisation did influence fungal beta diversity ($R^2 = 0.04$; $Pr(>F) = 0.002$) (Figure 5a; Table S6).

5 | DISCUSSION

We successfully promoted a brown rot outcome in all but one inoculated birch stem section, with all but one non-inoculated stem section having a white rot outcome. Broadening the range of rot-type outcomes was a significant accomplishment. *Fomitopsis betulina* was present as an endophyte in non-decayed stem sections we sampled, but it barely persisted in non-inoculated decaying birch, later to be dominated by white-rot fungal colonisers. This reflects the stress-tolerant life-history strategy of *F. betulina*, whereby it copes with strenuous abiotic conditions in a living tree to be among the first colonisers when the tree dies (Boddy & Griffith, 1989; Boddy & Hiscox, 2016). Cord-forming fungi in soil with combative life-history strategies may outcompete the early colonisers, such as *F. betulina* (Boddy, 2000; Boddy & Heilmann-Clausen, 2008), unless there is a significant inoculum potential to overcome invasion (Song et al., 2015). Our inoculum was enough to overcome invasion, with inoculated treatments having low variability and consistent dominance of *F. betulina*, excepting the one sample (E2) that became dominated by *Phanerochaete livescens*, showing all physicochemical signatures of white rot. Fast-growing white rot fungi from the soil (notably, *Phanerochaete*) colonised the stem sections lacking *F. betulina* inoculations when wood endophytes had been removed by sterilisation.

FIGURE 3 Fungal and bacterial compositions across treatments. Relative abundances of fungi (a) at the genus level and (b) as ecological groups. *Sistotrema* is marked as 'saprotroph' in the FungalTraits database (c) Relative abundances of bacteria at the phylum level. ''Non-decayed' refers to sound wood. Data for decayed samples are faceted horizontally by the soil variable (sterilised vs. non-sterilised) and vertically by the inoculum variable (inoculated vs. non-inoculated). The wood variable (sterilised vs. non-sterilised) is on the *x*-axes and the relative abundance of taxa/ecological groups (corresponding to different colours on the bar plots) is on the *y*-axes.


(a)
non-decayed
sterilised soil
non-sterilised soil
non-decayed
inoculated
non-inoculated
Relative Abundance (%)
100
75
50
25
0
non-decayed
sterilised
non-sterilised
wood
Unknown
Glomeromycota
Chytridiomycota
Rozellomycota
Mucoromycota
Mortierellomycota
Basidiomycota
Ascomycota
Phaeoacremonium
Pyrenopeziza
Trichoderma
Trametes
Peniophora
Phanerochaete
Sistotrema
Fomitopsis
(b)
unknown
unassigned
moss symbiont
yeast
lichenized
endophyte
mold
animal decomposer
ectomycorrhizal
fungal decomposer
plant pathogen
saprotroph
soft rot
white rot
brown rot
(c)
Fusobacteriota
Entotheonellaeota
Spirochaetota
Crenarchaeota
Latescibacterota
Nitrospirota
Deinococcota
Fibrobacterota
Sumerlaeota
Abditibacteriota
Dependentiae
Desulfobacterota
Cyanobacteria
Armatimonadota
Bdellovibrionota
Chloroflexi
Patescibacteria
Gemmatimonadota
Firmicutes
Myxococcota
Planctomycetota
Verrucomicrobiota
Bacteroidota
Acidobacteriota
Actinobacteriota
Proteobacteria

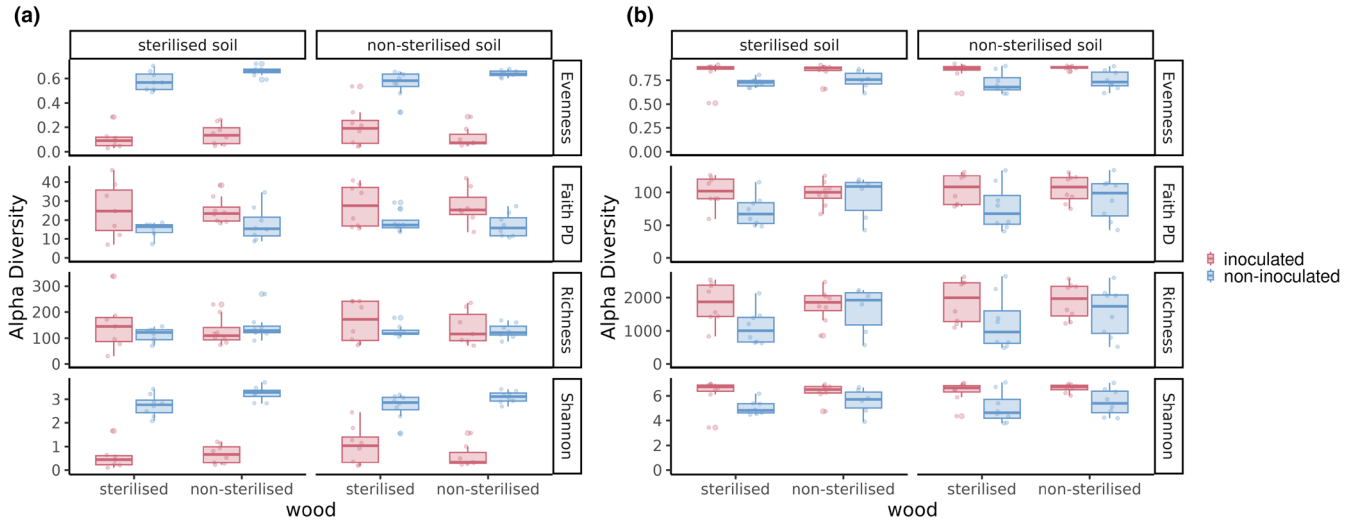


FIGURE 4 (a) Fungal and (b) bacterial alpha diversities in decayed samples across treatments. The data are faceted horizontally by the soil variable (sterilised vs. non-sterilised) and coloured by the inoculum variable (inoculated vs. non-inoculated). The wood variable (sterilised vs. non-sterilised) is on the *x*-axes and the alpha diversity values for the four metrics (faceted vertically) are on the *y*-axes.

Given similar density losses across non-inoculated (i.e., white-rotted) samples, variation in lignin degradation (apparent selectivity) was the primary driver of L:D differences, with highest lignin loss in treatments lacking wood pre-sterilisation. This may be due to lignin removal being higher when fungi decay pre-colonised wood, but it may simply be a consequence of the relative lignin-selectivity of the dominant strains (e.g., *Peniophora*) in the non-sterilised wood.

We hypothesised that if we could produce more brown rot in a portion of our decaying birch stem sections—thus broadening the range of rot-type outcomes—we could better test the functional consequences of rot types, such as changes in wood pH and sugar availability. This hypothesis was supported. A lower pH in brown-rotted than in white-rotted wood was not surprising, as pH broadly defines wood rot type (Cowling, 1961; Song et al., 2017). Carbohydrate concentrations, adjusted for density loss, were also different between rot types, with some variability, depending on white-rot fungal dominance. This difference likely reflects a fungal metabolic trade-off between removing lignin and releasing sugars. In monoculture studies, brown rot fungi release more free, soluble monosaccharides, compared to white rot fungi (Cowling, 1961; Schilling et al., 2015, 2020), likely due to a more random ROS depolymerisation strategy; however, this distinction is not seen in field samples with full microbial communities present (Jurgensen et al., 1989), potentially reflecting a bacterial 'cheater' role in metabolising excess soluble sugars (Allison, 2005).

We also hypothesised that more directed rot-type outcomes would establish clearer links between dominant fungi and codominant bacterial associates. We found a clear link between rot type and fungal dominance, but we did not find a parallel bacterial codominance. The increase in fungal richness observed post-decay aligns with previous findings (Christofides et al., 2019; Hoppe et al., 2015; Kubartová et al., 2012; Rajala et al., 2012, 2015), but we did not observe associations of white rot with Firmicutes or of brown rot with Acidobacteria, Actinobacteria and Alphaproteobacteria, as seen in standing dead birch (Haq et al., 2022). Moreover, bacterial alpha diversity (Shannon index) did not decrease with brown rot inoculations, as it did for fungi, and instead increased. Fungi may be directly modifying bacterial niche spaces by changing pH and/or sugar availability, as seen before (Haq et al., 2022; Hoppe et al., 2015; Johnston et al., 2019; Odriozola et al., 2021). 'Cheater' bacteria (Allison, 2005) might feed on soluble carbohydrates released by brown rot *F. betulina* due to its non-targeted ROS-based depolymerisation mechanism, and this might explain an increase in all four bacterial diversity metrics in *F. betulina*-dominated samples. Furthermore, bacteria 'stealing' sugars released during brown rot might be one of the factors that prevents brown rot fungi from dominating in field experiments (without the addition of exogenous inoculum) and limits their frequency and distribution in nature. However, a metagenomic follow-up to enhance resolution within the bacterial community could better reveal bacterial community differences between rot types, if any exist. Additionally, other prokaryotes and fungi (including yeasts) could be utilising the released sugars, shaping the success of brown rot.

One caveat to mention is the challenge of disentangling effects of density loss from those of rot type in a 14-month colonisation window. A faster brown rot decay mechanism, as seen under laboratory conditions (Castaño et al., 2018, 2022; Kleman-Leyer et al., 1992), could explain the differences in density losses between inoculated and non-inoculated samples. It seems more likely, however, that inoculated samples had more density loss due to greater fungal biomass (introduced via inoculation) and/or less competition with other species, including soft rot fungi in Ascomycota. We targeted decay classes II–III to restrict comparisons to the active decay window (Schilling et al., 2015) and adjusted lignin and carbohydrate concentrations to compensate for density loss (Anderson et al., 2023). However, we cannot similarly standardise microbial abundances

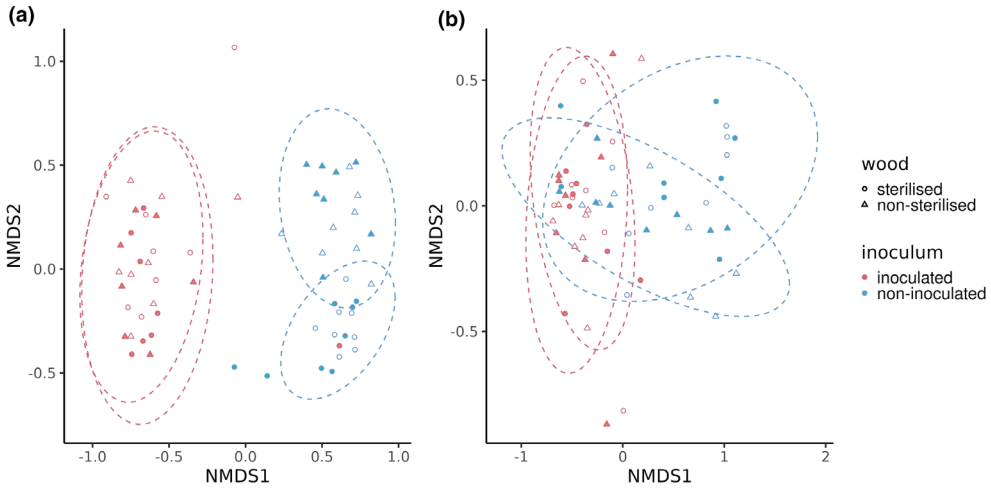


FIGURE 5 Non-metric multidimensional scaling plots of (a) fungal and (b) bacterial community composition, based on Bray–Curtis dissimilarity in decayed samples, across treatments. Circular shapes indicate samples with sterilised wood; triangular shapes indicate samples with non-sterilised wood. Pink shapes indicate inoculated samples; blue shapes indicate non-inoculated samples. Open shapes indicate samples placed on sterilised soil; closed shapes indicate samples placed on non-sterilised soil. Stress for plot (a) = 0.143; stress for plot (b) = 0.134.

and/or diversity indices. This caveat is shared with previous studies, where correlations between bacterial richness and density loss have included wood in all decay classes (I–V) (Harmon et al., 2008; Kielak et al., 2016; Rinta-Kanto et al., 2016), and results have varied (Hoppe et al., 2015; Kielak et al., 2016; Rinta-Kanto et al., 2016; Tláskal et al., 2017). We constrained variability by limiting the wood substrate to the same diameter, species, age, location of origin, plot for decay and soil-contact conditions, but there would be value in future work exploring the variability in each of these parameters, particularly given the colonisation success of other *Fomitopsis* species in early decay stages (Rajala et al., 2015).

One way we checked confounding effects of decay stage was by restricting analyses to an even narrower window of density losses where rot types overlapped. Comparing bacterial Shannon indices for three inoculated (i.e., brown-rotted) and three non-inoculated (i.e., white-rotted) samples in a density loss window of 19.6%–22.9% (Figure 1a,b), we still found that values differed, depending on rot type. Specifically, the bacterial Shannon index for three brown-rotted samples in this decay window averaged 6.41 ± 0.25, similar to the 6.19 ± 1.00 for all brown-rotted samples in decay stages II and III. The bacterial Shannon index for three white-rotted samples in this decay window averaged 5.80 ± 0.91, similar to the 5.55 ± 1.06 for all white-rotted samples in decay stages II and III. This suggests that rot type, not density loss, is driving distinct bacterial alpha diversities between inoculated and non-inoculated samples.

A second caveat relates to having multiple taxa compete for and dominate the white rot outcome, but only one, *F. betulina*, driving brown rot. In other words, species could be the main effect, not rot type, and our findings are constricted to a specific age class of birch stemwood. Some have found that ecological strategies of fungi influence associated bacterial communities, but that taxonomic identities do not (Johnston et al., 2019; Kielak et al., 2016). For example, an ability to form cords can translate to shifts in bacterial communities (Johnston et al., 2019), likely due to translocation of nitrogen and phosphorus from soil into wood substrates (Philpott et al., 2014). Others have shown abundances of certain fungal taxa to be better predictors of bacterial community composition than environmental predictors (Odriozola et al., 2021). If future work focuses on particular patterns emergent in our data, inoculating with more species would be logical.

Collectively, our study design effectively broadened the range of rot-type outcomes through the use of wood inoculations. We partially confirmed our hypothesis that these directed outcomes would enable clearer links between dominant fungi, their C release patterns, and their bacterial associates. A lack of relationship between rot-type dominance and bacterial codominance, along with negatively correlated fungal and bacterial diversity indices, was unexpected, suggesting that more niche space is available to bacteria when brown rot dominates wood decomposition. The ability to overcome site-specific colonisation pressure by controlling inoculum also provides more evidence for why simple growth parameters, such as hyphal extension rate (Lustenhouwer et al., 2020), can be useful predictors of decay *rates*. If combined with nutritional mode predictors of decay *fates* that are embedded as fungal traits in informatics pipelines, such as FungalTraits (Põlme et al., 2020), it suggests greater potential to predict C sequestration and release from wood as a function of biotic variability.

AUTHOR CONTRIBUTIONS

Aiym Bakytbaikyzy and Jonathan S. Schilling conceived the ideas and designed the methodology. Jonathan S. Schilling and Collin Adams carried out the fieldwork. Aiym Bakytbaikyzy processed the samples, performed physicochemical analyses, and carried out genomic DNA extractions. Aiym Bakytbaikyzy and Yanmei Zhang analysed

the data and interpreted the results. Aiym Bakytbaikyzy drafted the manuscript. Aiym Bakytbaikyzy, Jonathan S. Schilling, Yanmei Zhang and Collin Adams revised the manuscript. The final version was approved by all authors. All authors have agreed to be responsible for all aspects of the work to ensure that inquiries regarding accuracy or integrity are appropriately investigated and resolved.

ACKNOWLEDGEMENTS

This work was supported by Minnesota's Discovery, Research, and InnoVation Economy (MnDRIVE) Environment Graduate Scholar Seed Grant Award (Jonathan S. Schilling and Aiym Bakytbaikyzy) as well as the John Tester Itasca Research Fellowship (Aiym Bakytbaikyzy). The authors would also like to thank Itasca Biological Station and Laboratories at the College of Biological Sciences of the University of Minnesota for hosting visits and managing the plot area for this study.

CONFLICT OF INTEREST STATEMENT

The authors declare no conflict of interest.

DATA AVAILABILITY STATEMENT

All raw-sequencing data generated during the current study is uploaded to NCBI Sequence Read Archive repository (https://www.ncbi.nlm.nih.gov/sra) under study accession number PRJNA1198067. Data generated from physicochemical analyses are available in the Dryad Digital Repository: https://doi.org/10.5061/dryad.p8cz8wb3f (Bakytbaikyzy et al., 2025).

ORCID

Aiym Bakytbaikyzy https://orcid.org/0009-0006-7585-9639
Yanmei Zhang https://orcid.org/0009-0000-5210-9030
Jonathan S. Schilling https://orcid.org/0000-0003-0810-3007

REFERENCES

Abarenkov, K., Nilsson, R. H., Larsson, K.-H., Taylor, A. F. S., May, T. W., Frøslev, T. G., Pawlowska, J., Lindahl, B., Põldmaa, K., Truong, C., Vu, D., Hosoya, T., Niskanen, T., Piirmann, T., Ivanov, F., Zirk, A., Peterson, M., Cheeke, T. E., Ishigami, Y., … Kõljalg, U. (2024). The UNITE database for molecular identification and taxonomic communication of fungi and other eukaryotes: Sequences, taxa and classifications reconsidered. *Nucleic Acids Research*, *52*(D1), D791–D797. https://doi.org/10.1093/nar/gkad1039

Allison, S. D. (2005). Cheaters, diffusion and nutrients constrain decomposition by microbial enzymes in spatially structured environments. *Ecology Letters*, *8*(6), 626–635. https://doi.org/10.1111/j.1461-0248.2005.00756.x

Altschul, S. F., Gish, W., Miller, W., Myers, E. W., & Lipman, D. J. (1990). Basic local alignment search tool. *Journal of Molecular Biology*, *215*(3), 403–410. https://doi.org/10.1016/S0022-2836(05)80360-2

Anderson, C. E., Castaño, J. D., & Schilling, J. S. (2023). Fine-scale cation dynamics and control by *Rhodonia placenta* and *Pleurotus ostreatus* during wood decay. *International Biodeterioration & Biodegradation*, *183*, 105643. https://doi.org/10.1016/j.ibiod.2023.105643

Apps, M. J., Kurz, W. A., Luxmoore, R. J., Nilsson, L. O., Sedjo, R. A., Schmidt, R., Simpson, L. G., & Vinson, T. S. (1993). Boreal forests and tundra. *Water, Air, and Soil Pollution*, *70*(1), 39–53. https://doi.org/10.1007/BF01104987

Arantes, V., & Goodell, B. (2014). Current understanding of brown-rot fungal biodegradation mechanisms: A review. In *Deterioration and protection of sustainable biomaterials* (Vol. *1158*, pp. 3–21). American Chemical Society. https://doi.org/10.1021/bk-2014-1158.ch001

Bakytbaikyzy, A., Zhang, Y., Collins, A., & Schilling, J. S. (2025). Data from: Imposing primary colonisation success of wood-decomposing fungi in birch wood alters microbiome composition and carbon release rates. *Dryad Digital Repository*, https://doi.org/10.5061/dryad.p8cz8wb3f

Blanchette, R. (2003). Delignification by wood-decay fungi. *Annual Review of Phytopathology*, *29*, 381–403. https://doi.org/10.1146/annurev.py.29.090191.002121

Boddy, L. (2000). Interspecific combative interactions between wood-decaying basidiomycetes. *FEMS Microbiology Ecology*, *31*(3), 185–194. https://doi.org/10.1111/j.1574-6941.2000.tb00683.x

Boddy, L., & Griffith, G. S. (1989). Role of endophytes and latent invasion in the development of decay communities in sapwood of angiospermous trees. *Sydowia*, *41*, 41–73.

Boddy, L., & Heilmann-Clausen, J. (2008). Chapter 12: Basidiomycete community development in temperate angiosperm wood. *British Mycological Society Symposia Series*, *28*, 211–237. https://doi.org/10.1016/S0275-0287(08)80014-8

Boddy, L., & Hiscox, J. (2016). Fungal ecology: Principles and mechanisms of colonization and competition by saprotrophic fungi. *Microbiology Spectrum*, *4*(6). https://doi.org/10.1128/microbiolspec.funk-0019-2016

Callahan, B. J., McMurdie, P. J., Rosen, M. J., Han, A. W., Johnson, A. J. A., & Holmes, S. P. (2016). DADA2: High-resolution sample inference from Illumina amplicon data. *Nature Methods*, *13*(7), 581–583. https://doi.org/10.1038/nmeth.3869

Castaño, J. D., Muñoz-Muñoz, N., Kim, Y. M., Liu, J., Yang, L., & Schilling, J. S. (2022). Metabolomics highlights different life history strategies of white and Brown rot wood-degrading fungi. *M Sphere*, *7*(6), e00545-22. https://doi.org/10.1128/msphere.00545-22

Castaño, J. D., Zhang, J., Anderson, C. E., & Schilling, J. S. (2018). Oxidative damage control during decay of wood by Brown rot fungus using oxygen radicals. *Applied and Environmental Microbiology*, *84*(22), e01937-18. https://doi.org/10.1128/AEM.01937-18

Chen, H. (2014). Chemical composition and structure of natural lignocellulose. In H. Chen (Ed.), *Biotechnology of lignocellulose: Theory and practice* (pp. 25–71). Springer Netherlands. https://doi.org/10.1007/978-94-007-6898-7_2

Christofides, S. R., Hiscox, J., Savoury, M., Boddy, L., & Weightman, A. J. (2019). Fungal control of early-stage bacterial community development in decomposing wood. *Fungal Ecology*, *42*, 100868. https://doi.org/10.1016/j.funeco.2019.100868

Cline, L. C., Schilling, J. S., Menke, J., Groenhof, E., & Kennedy, P. G. (2018). Ecological and functional effects of fungal endophytes on wood decomposition. *Functional Ecology*, *32*(1), 181–191. https://doi.org/10.1111/1365-2435.12949

Cowling, E. B. (1961). *Comparative biochemistry of the decay of sweetgum sapwood by white-rot and brown-rot fungi*. U.S. Department of Agriculture.

de Boer, W., Folman, L. B., Summerbell, R. C., & Boddy, L. (2005). Living in a fungal world: Impact of fungi on soil bacterial niche development. *FEMS Microbiology Reviews*, *29*(4), 795–811. https://doi.org/10.1016/j.femsre.2004.11.005

Dickie, I. A., Fukami, T., Wilkie, J. P., Allen, R. B., & Buchanan, P. K. (2012). Do assembly history effects attenuate from species to ecosystem properties? A field test with wood-inhabiting fungi. *Ecology Letters*, *15*(2), 133–141. https://doi.org/10.1111/j.1461-0248.2011.01722.x

Floudas, D., Binder, M., Riley, R., Barry, K., Blanchette, R. A., Henrissat, B., Martínez, A. T., Otillar, R., Spatafora, J. W., Yadav, J. S., Aerts, A., Benoit, I., Boyd, A., Carlson, A., Copeland, A., Coutinho, P. M., De Vries, R. P., Ferreira, P., Findley, K., … Hibbett, D. S. (2012). The

Paleozoic origin of enzymatic lignin decomposition reconstructed from 31 fungal genomes. *Science*, *336*(6089), 1715–1719. https://doi.org/10.1126/science.1221748

Folman, L. B., Klein Gunnewiek, P. J. A., Boddy, L., & de Boer, W. (2008). Impact of white-rot fungi on numbers and community composition of bacteria colonizing beech wood from forest soil. *FEMS Microbiology Ecology*, *63*(2), 181–191. https://doi.org/10.1111/j.1574-6941.2007.00425.x

Friedlingstein, P., Jones, M. W., O'Sullivan, M., Andrew, R. M., Bakker, D. C. E., Hauck, J., Le Quéré, C., Peters, G. P., Peters, W., Pongratz, J., Sitch, S., Canadell, J. G., Ciais, P., Jackson, R. B., Alin, S. R., Anthoni, P., Bates, N. R., Becker, M., Bellouin, N., … Zeng, J. (2022). Global carbon budget 2021. *Earth System Science Data*, *14*(4), 1917–2005. https://doi.org/10.5194/essd-14-1917-2022

Fukami, T., Dickie, I. A., Paula Wilkie, J., Paulus, B. C., Park, D., Roberts, A., Buchanan, P. K., & Allen, R. B. (2010). Assembly history dictates ecosystem functioning: Evidence from wood decomposer communities: Carbon dynamics and fungal community assembly. *Ecology Letters*, *13*(6), 675–684. https://doi.org/10.1111/j.1461-0248.2010.01465.x

Gilbertson, R. L. (1980). Wood-rotting fungi of North America. *Mycologia*, *72*(1), 1–49. https://doi.org/10.1080/00275514.1980.12021153

Gohl, D. M., Vangay, P., Garbe, J., MacLean, A., Hauge, A., Becker, A., Gould, T. J., Clayton, J. B., Johnson, T. J., Hunter, R., Knights, D., & Beckman, K. B. (2016). Systematic improvement of amplicon marker gene methods for increased accuracy in microbiome studies. *Nature Biotechnology*, *34*(9), 942–949. https://doi.org/10.1038/nbt.3601

Haq, I. U., Hillmann, B., Moran, M., Willard, S., Knights, D., Fixen, K. R., & Schilling, J. S. (2022). Bacterial communities associated with wood rot fungi that use distinct decomposition mechanisms. *ISME Communications*, *2*(1), 26. https://doi.org/10.1038/s43705-022-00108-5

Harmon, M. E., Franklin, J. F., Swanson, F. J., Sollins, P., Gregory, S. V., Lattin, J. D., Anderson, N. H., Cline, S. P., Aumen, N. G., Sedell, J. R., Lienkaemper, G. W., Cromack, K., & Cummins, K. W. (2004). Ecology of Coarse Woody Debris in temperate ecosystems. *Advances in Ecological Research*, *34*, 59–234. https://doi.org/10.1016/S0065-2504(03)34002-4

Harmon, M. E., Woodall, C. W., Fasth, B., & Sexton, J. (2008). *Woody detritus density and density reduction factors for tree species in the United States: A synthesis* (No. NRS-GTR-29; p. NRS-GTR-29). U.S. Department of Agriculture, Forest Service, Northern Research Station. https://doi.org/10.2737/NRS-GTR-29

Henningsson, B. (1965). *Physiology and decay activity of the birch conk fungus Polyporus betulinus (Bull.) Fr.* Skogshögskolan.

Hoppe, B., Krüger, D., Kahl, T., Arnstadt, T., Buscot, F., Bauhus, J., & Wubet, T. (2015). A pyrosequencing insight into sprawling bacterial diversity and community dynamics in decaying deadwood logs of *Fagus sylvatica* and *Picea abies*. *Scientific Reports*, *5*(1), 9456. https://doi.org/10.1038/srep09456

Houghton, R. A., Hall, F., & Goetz, S. J. (2009). Importance of biomass in the global carbon cycle. *Journal of Geophysical Research: Biogeosciences*, *114*(G2), 2009JG000935. https://doi.org/10.1029/2009JG000935

Janeš, D., Umek, A., & Kreft, S. (2006). Evaluation of antibacterial activity of extracts of five species of wood-colonizing fungi. *Journal of Basic Microbiology*, *46*(3), 203–207. https://doi.org/10.1002/jobm.200510035

Johnston, S. R., Boddy, L., & Weightman, A. J. (2016). Bacteria in decomposing wood and their interactions with wood-decay fungi. *FEMS Microbiology Ecology*, *92*(11), 1–12. https://doi.org/10.1093/femsec/fiw179

Johnston, S. R., Hiscox, J., Savoury, M., Boddy, L., & Weightman, A. J. (2019). Highly competitive fungi manipulate bacterial communities in decomposing beech wood (*Fagus sylvatica*). *FEMS Microbiology Ecology*, *95*(2), fiy225. https://doi.org/10.1093/femsec/fiy225

Jurgensen, M. F., Larsen, M. J., Wolosiewicz, M., & Harvey, A. E. (1989). A comparison of dinitrogen fixation rates in wood litter decayed by white-rot and brown-rot fungi. *Plant and Soil*, *115*(1), 117–122. https://doi.org/10.1007/BF02220701

Keenan, T. F., Davidson, E. A., Munger, J. W., & Richardson, A. D. (2013). Rate my data: Quantifying the value of ecological data for the development of models of the terrestrial carbon cycle. *Ecological Applications*, *23*(1), 273–286. https://doi.org/10.1890/12-0747.1

Kembel, S. W., Cowan, P. D., Helmus, M. R., Cornwell, W. K., Morlon, H., Ackerly, D. D., Blomberg, S. P., & Webb, C. O. (2010). Picante: R tools for integrating phylogenies and ecology. *Bioinformatics*, *26*(11), 1463–1464. https://doi.org/10.1093/bioinformatics/btq166

Kielak, A. M., Scheublin, T. R., Mendes, L. W., van Veen, J. A., & Kuramae, E. E. (2016). Bacterial community succession in pine-wood decomposition. *Frontiers in Microbiology*, *7*, 231. https://doi.org/10.3389/fmicb.2016.00231

Kleman-Leyer, K., Agosin, E., Conner, A. H., & Kirk, T. K. (1992). Changes in molecular size distribution of cellulose during attack by white rot and brown rot fungi. *Applied and Environmental Microbiology*, *58*(4), 1266–1270. https://doi.org/10.1128/aem.58.4.1266-1270.1992

Kneeshaw, D., & Gauthier, S. (2003). Old growth in the boreal forest: A dynamic perspective at the stand and landscape level. *Environmental Reviews*, *11*(S1), S99–S114. https://doi.org/10.1139/a03-010

Kubartová, A., Ottosson, E., Dahlberg, A., & Stenlid, J. (2012). Patterns of fungal communities among and within decaying logs, revealed by 454 sequencing. *Molecular Ecology*, *21*(18), 4514–4532. https://doi.org/10.1111/j.1365-294X.2012.05723.x

Kubicek, C. P., Herrera-Estrella, A., Seidl-Seiboth, V., Martinez, D. A., Druzhinina, I. S., Thon, M., Zeilinger, S., Casas-Flores, S., Horwitz, B. A., Mukherjee, P. K., Mukherjee, M., Kredics, L., Alcaraz, L. D., Aerts, A., Antal, Z., Atanasova, L., Cervantes-Badillo, M. G., Challacombe, J., Chertkov, O., … Grigoriev, I. V. (2011). Comparative genome sequence analysis underscores mycoparasitism as the ancestral life style of Trichoderma. *Genome Biology*, *12*(4), R40. https://doi.org/10.1186/gb-2011-12-4-r40

Lahti, L., & Shetty, S. (2017). *Microbiome R package*. https://doi.org/10.18129/B9.bioc.microbiome

Lodge, D. J. (1997). Factors related to diversity of decomposer fungi in tropical forests. *Biodiversity and Conservation*, *6*(5), 681–688. https://doi.org/10.1023/A:1018314219111

López-Mondéjar, R., Zühlke, D., Becher, D., Riedel, K., & Baldrian, P. (2016). Cellulose and hemicellulose decomposition by forest soil bacteria proceeds by the action of structurally variable enzymatic systems. *Scientific Reports*, *6*(1), 25279. https://doi.org/10.1038/srep25279

Lustenhouwer, N., Maynard, D. S., Bradford, M. A., Lindner, D. L., Oberle, B., Zanne, A. E., & Crowther, T. W. (2020). A trait-based understanding of wood decomposition by fungi. *Proceedings of the National Academy of Sciences of the United States of America*, *117*(21), 11551–11558. https://doi.org/10.1073/pnas.1909166117

Maillard, F., Jusino, M. A., Andrews, E., Moran, M., Vaziri, G. J., Banik, M. T., Fanin, N., Trettin, C. C., Lindner, D. L., & Schilling, J. S. (2022). Wood-decay type and fungal guild dominance across a North American log transplant experiment. *Fungal Ecology*, *59*, 101151. https://doi.org/10.1016/j.funeco.2022.101151

Martin, A. R., Domke, G. M., Doraisami, M., & Thomas, S. C. (2021). Carbon fractions in the world's dead wood. *Nature Communications*, *12*(1), 889. https://doi.org/10.1038/s41467-021-21149-9

Murray, A. C., & Woodward, S. (2003). In vitro interactions between bacteria isolated from Sitka spruce stumps and *Heterobasidion annosum*. *Forest Pathology*, *33*(1), 53–67. https://doi.org/10.1046/j.1439-0329.2003.00307.x

Odriozola, I., Abrego, N., Tláskal, V., Zrůstová, P., Morais, D., Větrovský, T., Ovaskainen, O., & Baldrian, P. (2021). Fungal communities are important determinants of bacterial community composition in deadwood. *MSystems*, *6*(1), e01017-20. https://doi.org/10.1128/msystems.01017-20

Oksanen, J., Blanchet, F. G., Friendly, M., Kindt, R., Legendre, P., McGlinn, D., Minchin, P., O'Hara, R., Simpson, G., Solymos, P., Stevens, H., Szöcs, E., & Wagner, H. (2017). *vegan: Community ecology package*. Ordination methods, diversity analysis and other functions for community and vegetation ecologists. Version 2.4-3. https://CRAN.R-project.org/package=vegan

Pettersen, R. C. (1984). The chemical composition of wood. In R. Rowell (Ed.), *The chemistry of solid wood* (p. 76). American Chemical Society.

Philpott, T. J., Prescott, C. E., Chapman, W. K., & Grayston, S. J. (2014). Nitrogen translocation and accumulation by a cord-forming fungus (*Hypholoma fasciculare*) into simulated woody debris. *Forest Ecology and Management*, *315*, 121–128. https://doi.org/10.1016/j.foreco.2013.12.034

Pierce, E. C., Morin, M., Little, J. C., Liu, R. B., Tannous, J., Keller, N. P., Pogliano, K., Wolfe, B. E., Sanchez, L. M., & Dutton, R. J. (2021). Bacterial–fungal interactions revealed by genome-wide analysis of bacterial mutant fitness. *Nature Microbiology*, *6*(1), 87–102. https://doi.org/10.1038/s41564-020-00800-z

Pleszczyńska, M., Lemieszek, M. K., Siwulski, M., Wiater, A., Rzeski, W., & Szczodrak, J. (2017). Fomitopsis betulina (formerly *Piptoporus betulinus*): The Iceman's polypore fungus with modern biotechnological potential. *World Journal of Microbiology and Biotechnology*, *33*(5), 83. https://doi.org/10.1007/s11274-017-2247-0

Põlme, S., Abarenkov, K., Henrik Nilsson, R., Lindahl, B. D., Clemmensen, K. E., Kauserud, H., Nguyen, N., Kjøller, R., Bates, S. T., Baldrian, P., Frøslev, T. G., Adojaan, K., Vizzini, A., Suija, A., Pfister, D., Baral, H.-O., Järv, H., Madrid, H., Nordén, J., … Tedersoo, L. (2020). FungalTraits: A user-friendly traits database of fungi and fungus-like stramenopiles. *Fungal Diversity*, *105*(1), 1–16. https://doi.org/10.1007/s13225-020-00466-2

Quast, C., Pruesse, E., Yilmaz, P., Gerken, J., Schweer, T., Yarza, P., Peplies, J., & Glöckner, F. O. (2013). The SILVA ribosomal RNA gene database project: Improved data processing and web-based tools. *Nucleic Acids Research*, *41*(D1), D590–D596. https://doi.org/10.1093/nar/gks1219

Rajala, T., Peltoniemi, M., Pennanen, T., & Mäkipää, R. (2012). Fungal community dynamics in relation to substrate quality of decaying Norway spruce (*Picea abies* [L.] Karst.) logs in boreal forests. *FEMS Microbiology Ecology*, *81*(2), 494–505. https://doi.org/10.1111/j.1574-6941.2012.01376.x

Rajala, T., Tuomivirta, T., Pennanen, T., & Mäkipää, R. (2015). Habitat models of wood-inhabiting fungi along a decay gradient of Norway spruce logs. *Fungal Ecology*, *18*, 48–55. https://doi.org/10.1016/j.funeco.2015.08.007

Rayner, A., & Boddy, L. (1988). Fungal decomposition of wood. Its biology and ecology. In *Fungal decomposition of wood. Its biology and ecology*. John Wiley & Sons Ltd.; CABI Databases.

Rinta-Kanto, J. M., Sinkko, H., Rajala, T., Al-Soud, W. A., Sørensen, S. J., Tamminen, M. V., & Timonen, S. (2016). Natural decay process affects the abundance and community structure of bacteria and archaea in Picea abies logs. *FEMS Microbiology Ecology*, *92*(7), fiw087. https://doi.org/10.1093/femsec/fiw087

Rousk, J., Demoling, L. A., Bahr, A., & Bååth, E. (2008). Examining the fungal and bacterial niche overlap using selective inhibitors in soil. *FEMS Microbiology Ecology*, *63*(3), 350–358. https://doi.org/10.1111/j.1574-6941.2008.00440.x

Salvachúa, D., Karp, E. M., Nimlos, C. T., Vardon, D. R., & Beckham, G. T. (2015). Towards lignin consolidated bioprocessing: Simultaneous lignin depolymerization and product generation by bacteria. *Green Chemistry*, *17*(11), 4951–4967. https://doi.org/10.1039/C5GC01165E

Schilling, J. S., Kaffenberger, J. T., Held, B. W., Ortiz, R., & Blanchette, R. A. (2020). Using wood rot phenotypes to illuminate the "gray" among decomposer fungi. *Frontiers in Microbiology*, *11*(June), 1–12. https://doi.org/10.3389/fmicb.2020.01288

Schilling, J. S., Kaffenberger, J. T., Liew, F. J., & Song, Z. (2015). Signature wood modifications reveal decomposer community history. *PLoS One*, *10*(3), e0120679. https://doi.org/10.1371/journal.pone.0120679

Schubert, M., Fink, S., & Schwarze, F. W. M. R. (2008). Evaluation of *Trichoderma* spp. As a biocontrol agent against wood decay fungi in urban trees. *Biological Control*, *45*(1), 111–123. https://doi.org/10.1016/j.biocontrol.2008.01.001

Simpson, H. J., Andrew, C., Skrede, I., Kauserud, H., & Schilling, J. S. (2024). Global field collection data confirm an affinity of brown rot fungi for coniferous habitats and substrates. *New Phytologist*, *242*(6), 2775–2786. https://doi.org/10.1111/nph.19723

Song, Z., Kennedy, P. G., Liew, F. J., & Schilling, J. S. (2017). Fungal endophytes as priority colonizers initiating wood decomposition. *Functional Ecology*, *31*(2), 407–418. https://doi.org/10.1111/1365-2435.12735

Song, Z., Vail, A., Sadowsky, M. J., & Schilling, J. S. (2015). Influence of hyphal inoculum potential on the competitive success of fungi colonizing wood. *Microbial Ecology*, *69*(4), 758–767. https://doi.org/10.1007/s00248-015-0588-5

Stokland, J., & Alfredsen, G. (2024). From deadwood to forest soils: Quantifying a key carbon flux in boreal ecosystems. *Biogeochemistry*, *167*, 1225–1242. https://doi.org/10.1007/s10533-024-01170-y

Stopnisek, N., Zühlke, D., Carlier, A., Barberán, A., Fierer, N., Becher, D., Riedel, K., Eberl, L., & Weisskopf, L. (2016). Molecular mechanisms underlying the close association between soil Burkholderia and fungi. *The ISME Journal*, *10*(1), 253–264. https://doi.org/10.1038/ismej.2015.73

Stutz, K. P., Dann, D., Wambsganss, J., Scherer-Lorenzen, M., & Lang, F. (2017). Phenolic matter from deadwood can impact forest soil properties. *Geoderma*, *288*, 204–212. https://doi.org/10.1016/j.geoderma.2016.11.014

Stutz, K. P., Kaiser, K., Wambsganss, J., Santos, F., Berhe, A. A., & Lang, F. (2019). Lignin from white-rotted European beech deadwood and soil functions. *Biogeochemistry*, *145*(1), 81–105. https://doi.org/10.1007/s10533-019-00593-2

Tláskal, V., Brabcová, V., Větrovský, T., Jomura, M., López-Mondéjar, R., Oliveira Monteiro, L. M., Saraiva, J. P., Human, Z. R., Cajthaml, T., Nunes da Rocha, U., & Baldrian, P. (2021). Complementary roles of wood-inhabiting fungi and bacteria facilitate deadwood decomposition. *mSystems*, *6*(1), e01078-20. https://doi.org/10.1128/msystems.01078-20

Tláskal, V., Zrůstová, P., Vrška, T., & Baldrian, P. (2017). Bacteria associated with decomposing dead wood in a natural temperate forest. *FEMS Microbiology Ecology*, *93*(12), fix157. https://doi.org/10.1093/femsec/fix157

Van Der Wal, A., Ottosson, E., & De Boer, W. (2015). Neglected role of fungal community composition in explaining variation in wood decay rates. *Ecology*, *96*(1), 124–133. https://doi.org/10.1890/14-0242.1

Worrall, J. J., Anagnost, S. E., & Zabel, R. A. (1997). Comparison of wood decay among diverse lignicolous fungi. *Mycologia*, *89*(2), 199–219. https://doi.org/10.1080/00275514.1997.12026772

Yelle, D. J., Ralph, J., Lu, F., & Hammel, K. E. (2008). Evidence for cleavage of lignin by a brown rot basidiomycete. *Environmental Microbiology*, *10*(7), 1844–1849. https://doi.org/10.1111/j.1462-2920.2008.01605.x

Zhang, Y., Song, Z., & Schilling, J. S. (2024). Evaluation of DNA extraction methods for microbial community profiling in deadwood decomposition. *MicrobiologyOpen*, *13*(6), e70007. https://doi.org/10.1002/mbo3.70007

SUPPORTING INFORMATION

Additional supporting information can be found online in the Supporting Information section at the end of this article.

Figure S1. The workflow of how birch stem sections were prepared for the experiment and sectioned at harvest.

Figure S2. Surface-area-to-volume ratios of birch sections post-decay.

Figure S3. Fungal and bacterial alpha diversities (richness, Pielou evenness index, Shannon index and Faith PD index) in non-decayed vs decayed samples.

Figure S4. Non-metric multidimensional scaling (NMDS) plots of fungal and bacterial community composition based on Bray–Curtis dissimilarity in non-decayed vs decayed samples.

Figure S5. Relative abundances of fungi at the genus level, showing all replicates.

Table S1. Experimental design.

Table S2. Information on primers used for amplicon sequencing, targeting ITS2 and 16S rRNA V4 genes.

Table S3. Amounts of structural carbohydrates and Klason (i.e., acid-insoluble) lignin in samples.

Table S4. Results of statistical tests performed to compare values for fungal communities' alpha diversity metrics in non-decayed vs decayed samples.

Table S5. Results of statistical tests performed to compare values for fungal and bacterial communities' alpha diversity metrics in inoculated vs non-inoculated samples.

Table S6. Fungal and bacterial communities' beta diversity metrics in decayed samples.

How to cite this article: Bakytbaikyzy, A., Zhang, Y., Adams, C., & Schilling, J. S. (2025). Imposing primary colonisation success of wood-decomposing fungi in birch wood alters microbiome composition and carbon release rates. *Functional Ecology*, *39*, 2690–2703. https://doi.org/10.1111/1365-2435.70148